Paper
Int'l J. of Aeronautical & Space Sci. 18(3), 395–402 (2017)
DOI: http://dx.doi.org/10.5139/IJASS.2017.18.3.395

Heat Transfer and Frictions in the Convergent/divergent Channel with Λ/V-shaped Ribs on Two Walls

Beom-soo Kim*

Department of Mechanical and System Engineering, Gyeongsang National University, Tongyeong 53064, Republic of Korea

Myung-sung Lee**

Evaluation Team, Gyeongnam Institute for Regional Program Evaluation, Changwon 51401, Republic of Korea

Soo-whan Ahn***

Department of Mechanical and System Engineering, Institute of Marine Industry, Gyeongsang National University, Tongyeong 53064, Republic of Korea

Abstract

The local heat transfer and total pressure drops of developed turbulent flows in the ribbed rectangular convergent/divergent channels with Λ/V-shaped ribs have been investigated experimentally. The channels have the exit hydraulic diameter (D_{ho}) to inlet hydraulic diameter (D_{hi}) ratios of 0.67 for convergence and 1.49 for divergence, respectively. The Λ/V-shaped ribs with three different flow attack angles of 30°, 45°, and 60° are manufactured with a fixed rib height (e) of 10 mm and the ratio of rib spacing (S) to height (e) of 10 on the walls. Thermal performances of the ribbed rectangular convergent/divergent channels are compared with the smooth straight tube under identical pumping power. The results show that the flow attack angle of 45° with Λ-shaped rib has the greatest thermal performance at all the Reynolds numbers studied in the convergent channel; whereas, the flow attack angle of 60° with V-shaped rib has the greatest thermal performance over Reynolds number of 30,000 in the divergent channel.

Key words: Ribbed rectangular convergent/divergent channel, Λ/V-shaped ribs, Flow attack angle, Heat transfer, Total pressure drop, Thermal performance

1. Introduction

Casting turbulence promoters/ribs inside cooling passages are an effective technique to augment the heat transfer rate inside turbine blades. The ribs break the laminar sublayer of turbulent flow due to flow separation and reattachment in the opposite near wall region of the cooling channels. Thus, the cooling effect is enormously improved. The experimental studies of effects of rib configurations (such as rib height, spacing, angle of attack) and flow Reynolds numbers on the heat transfer and friction factors for the fully developed region in a uniformly heated rectangular straight channel with rib-roughened walls along streamwise distance were systematically performed[1, 2].

The inclination of rib was found to yield superior heat transfer performance because of the secondary flow induced by the rib angle. This secondary flow has the form of two counter-rotating vortices, aligned with the inclined ribs on two opposite walls, which carry the cold fluid from the central core region towards the ribbed walls. These cells, interacting with the main flow, affect the flow reattachment and recirculation between ribs, and interrupt boundary layer

* Associate Professor
** Researcher
*** Full Professor, Corresponding author: asw9294@naver.com

Received: December 20, 2016 Revised: August 2, 2017 Accepted: August 2, 2017

growth downstreams of the reattachment regions.

The study of heat transfer performance of square channels with angled ribs drew the guidelines for the appropriate thermal design of a channel with angled ribs. In straight square channels ribbed on two opposite walls and smooth on the other walls with S/e=10 -20 and e/D_h=0.063, the greatest Nu, accompanied by the greatest f, occurred at a rib angle-of-attack α between 60° and 75°, whereas the best performance for a constant pumping power occurred at an angle-of-attack between 30° and 45°[3].

Han et al. [4] examined the effects of the rib angle orientations on the local, regionally averaged heat transfer distributions and pressure drops in square straight channels with 12 different rib arrangements on two opposite walls. The results show that the continuous V-shaped ribs do better than the continuous angled parallel ribs or transverse parallel ribs. This is because the V-shaped continuous rib induces a four-cell secondary flow while the parallel continuous rib has a two-cell secondary flow, in addition to breaking the laminar sublayer in the opposite near wall region of the cooling channel.

However, no significant researches are presented in the existing literature that has reported the heat transfer and friction factor in the convergent/divergent channel with ribs on the wall. Lee et al. [5] conducted the experimental study on the local heat transfer and pressure drop of fully developed flow in the stationary ribbed rectangular convergent/divergent channel.

The rectangular convergent/divergent channel with one-sided ribbed surface only has the wall inclination angles of 0.72° and 1.43° at which the ribbed wall is manufactured with a fixed rib height e =10 mm and the ratio of rib spacing (S) to height (e) =10. The result shows that, among the four channels of D_{ho}/D_{hi}= 0.67, 0.86, 1.16 and 1.49, the divergent channel of D_{ho}/D_{hi} =1.49 has the greatest thermal performance at the identical mass flow rate, and the divergent channel of D_{ho}/D_{hi} =1.16 has the greatest at the identical pumping power.

Lee and Ahn [6] measured the effect of rib spacing (S) to height (e) on total friction factor and heat transfer results for the fully developed regime in the ribbed divergent channel. The ribbed divergent rectangular channel with the exit hydraulic diameter (D_{ho}) to inlet hydraulic diameter (D_{hi}) ratio of 1.16 corresponding to wall inclination angle of 0.72 deg and the rib spacing (S) to height (e) ratios of 6, 10, and 14 are considered.

Effects of angled ribs on the turbulent heat transfer and friction factors in a rectangular divergent channel were also presented [7].

Four different divergent channel with parallel angled ribs (α=30°, 45°, 60° and 90°) are placed to the channel's two opposite walls as well as the channel's one-sided wall only, respectively. The ribbed rectangular divergent channel has the inclination angle of 0.72° at the left and right walls, corresponding to D_{ho}/D_{hi} =1.16 having the cross section of 100 × 75 mm² at inlet and 100 × 100 mm² at exit.

They concluded that, for the identical mass flow rate, the two opposite 90° parallel rib angled wall channel has the highest thermal performance, whereas, for the identical pumping power and pressure drop, the two opposite 45° parallel rib angled wall channel has the greatest thermal performance over the Reynolds number of 60,000.

In this paper, local heat transfer coefficient and friction characteristics in a rib-roughened rectangular convergent/divergent channels with three different angled Λ/V-shaped ribs (α=30°, 45° and 60°) are presented. Configurations include sequences of Λ/V-shaped ribs, having cross sections of 100 × 100 mm² at inlet and 100 × 50 mm² at exit in the convergent channel (D_{ho}/D_{hi} =0.67); whereas, 100 × 50 mm² at inlet and 100 × 100 mm² at exit in the divergent channel (D_{ho}/D_{hi} =1.49). The ribs with height (e) of 10 mm are regularly spaced over two opposite sides and heated at uniform heat flux (the other sides remaining smooth and unheated).

2. Apparatus

The experimental setup is described in some details [5, 6]. A schematic drawing of the experimental system is presented in Fig. 1. The system is an open test loop, with the room air being drawn by a blower. The forced air goes through a honeycomb with a 2,500-mm-long entrance section, a test section of 1,000 mm, and a 3-inch diameter and 800-mm-long pipe equipped with a multiport average pitot tube to measure the flow bulk velocity.

The rectangular convergent channel has the cross section of 100 × 100 mm² at inlet and 100 × 50 mm² at exit; whereas, the divergent channel has the cross section of 100 × 50 mm² at inlet and 100 × 100 mm² at exit. The rectangular convergent/divergent channel has the inclination angle of +1.43°/-1.43° along the streamwise distance. The inclined left and right side walls with ribs are heated and the straight top

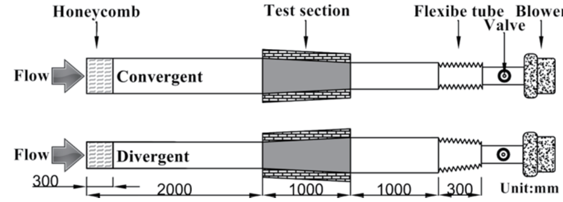

Fig. 1. Experimental apparatus

and bottom smooth walls are insulated.

The rib arrangements having three different flow attack angles with a rib height (e) =10 mm and the rib spacing (S) of 100 mm are shown in Fig. 2.

The copper plate method (in which each wall in the channel is divided into multiple regions comprising one high conductivity copper plate each) has been employed. In this study, each of the two walls is subdivided into 10 subsequential streamwise regions, comprised of 1 copper plate (100 × 100 mm^2) each. Ribs are made of copper and attached to the copper plates by using 0.02-mm-thick double sided tape to ensure thermal contact.

Some ribs do cross over from one region to the next region and might create a conductive path for heat to flow from one region to another. This effect is neglected in data reduction, as the effect is expected to be minor.

The 0.1-mm-thick silicone etched type heaters are glued to the back of each surface (left and right). The thermocouple junctions are heated between two subsequent ribs. The T-type copper-constantant thermocouples are buried inside a 0.4-mm-dia-hole drilled on the plate and held in place by using an epoxy resin. These thermocouples connected to Yokogawa DA100. The test section is installed in a 50-mm-thick pine wood housing. Further insulation is provided by encapsulating the entire test section in a thick layer of glass wool.

12 pressure taps are set up at the same interval along the top smooth center line for measuring the static pressure drop. Static pressure is measured by using a digital manometer with a resolution up to 0.01 mm H_2O at the static pressure of 19.99 mmH_2O, depending on its value.

The maximum wall temperature was less than about 90°C, and the maximum temperature drop between the duct outlet and the inlet was less than 22°C. The measurement was conducted within the range of Reynolds numbers from 22,000 to 75,000.

The inlet air temperature was measured by a thermocouple checked by a thermometer with a resolution of 0.1°C. The bulk temperature of the exiting air was measured by five thermocouples distributed at different vertical locations of the outlet cross section. The thermocouples were calibrated in advance and their accuracy was estimated to be about 0.2 °C.

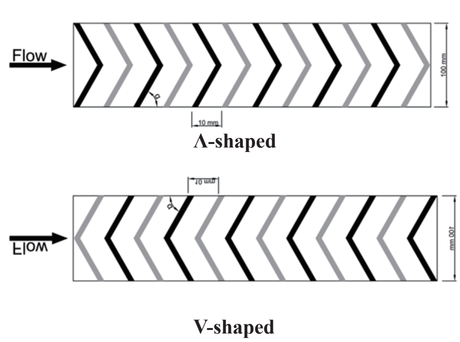

Fig. 2. Λ/V-shaped ribs on the left and right walls

The thermocouples were calibrated in advance and the accuracy was estimated to be about 0.2°C. An uncertainty estimation was conducted as suggested by Kline and McClintock [8].

3. Data Reduction

The local heat transfer coefficient h obtained from the net heat transfer rate (Q-Q_{loss}), the difference between the local wall temperature, and the local bulk mean air temperature is defined as,

$$h = \frac{(Q - Q_{loss})}{A_x(T_{wx} - T_{bx})}, \qquad (1)$$

where A_x means the projected heat transfer area from the inlet to the thermocouple junction at the ribbed wall. The heat loss to the environment is determined by a heat loss test. The test section (with all insulation in place and its interior filled with fiberglass) is heated until a steady state temperature is reached. The heat supplied at steady state is equal to the heat leakage through the external insulation. This test is performed for two steady temperatures, corresponding to the lowest and greatest temperatures expected in the experiment. Typical heat loss values are roughly 4-6% of the total heat supplied. The channel average Nusselt number (Nu) is defined as,

$$Nu = \frac{\bar{h} D_h}{k}, \qquad (2)$$

where D_h is $(D_{hi}+D_{ho})/2$. $\bar{h}$ stands for the channel average heat transfer coefficient. The Reynolds number is defined as,

$$Re = \frac{u_b D_h}{\nu}, \qquad (3)$$

where u_b is the channel average velocity. The total friction factor of the divergent channel is defined as,

$$f_T = \frac{D_h}{2\rho u_b^2}\left|\frac{\Delta P_T}{L}\right|, \qquad (4)$$

where the total pressure difference ΔP_T stands for P_i - $P_o + \frac{1}{2}\rho u_{bi}^2$ - $\frac{1}{2}\rho u_{bo}^2$. L is the length of test section.

The subscripts i and o are the inlet and exit of test section, respectively. The measured results may be regarded as some representatively reflecting the effects of the Λ/V-shaped ribs with three different flow attack angles on the heat transfer and total pressure drop behavior.

4. Experimental Results

A set of total pressure drops for the convergent (D_{ho}/D_{hi} =0.67)/divergent (D_{ho}/D_{hi} =1.49) rectangular channels with three different angles (30°, 40°, and 60°) on two opposite Λ/V-shaped ribbed walls are indicated in Fig. 3. This figure reveals in the convergent channel that the negative (-) total pressure drops (ΔP_T) were produced in all cases. This is the contrary to the public opinion that the flow direction is determined from the pressure drop difference along the streamwise distance; whereas, the positive (+) total pressure drop in the divergent channel was attributed to the fact that the increased magnitude of dynamic pressure drop ($\rho\frac{u_{bi}^2}{2} - \rho\frac{u_{bo}^2}{2}$) by augmented cross-sectional area along the streamwise distance is greater than the reduced magnitude of static pressure drop (P_i-P_o).

The increase in the total pressure drops for the flow attack angles can be seen in the order of 45°, 60°, and 30° in the ribbed convergent rectangular channel; whereas, in the order 30°, 45°, and 60° in the ribbed divergent channel. It is reasoned from the definition of total pressure drop.

Figure 4 is the total friction factors obtained from Eq.(4), along with results by our previous work [7] in the divergent channel of D_{ho}/D_{hi} =1.49.

The increase in the total friction factors can be seen in the order of 45°, 60°, and 30° in the ribbed convergent channel; whereas, 30°, 45° and 60° in the ribbed divergent channel.

The friction factor f_{ss} for the fully developed turbulent flow in the smooth straight circular tube suggested by Blasius [9] is presented as a reference (dotted line).

The interesting feature of the total friction factors of this paper can be seen that, on the contrary to the public opinion, the total friction factors of 60° with V-shaped ribs in the divergent channel (solid triangle symbols) are somewhat similar to those for what was suggested by Blasius for the smooth straight circular tube. It is possible that the decrease in the static pressure drop is induced by the ribbed divergent walls.

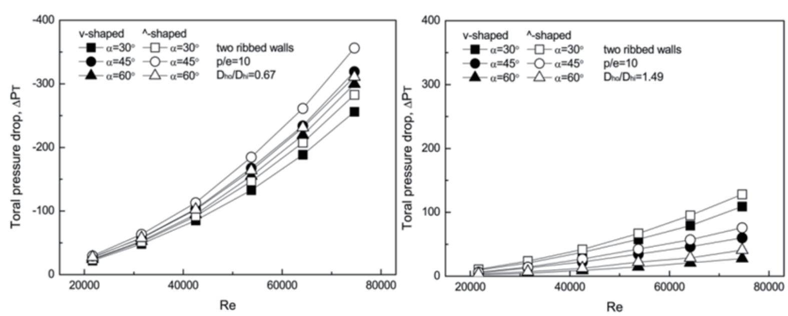

Fig. 3. Total pressure drops

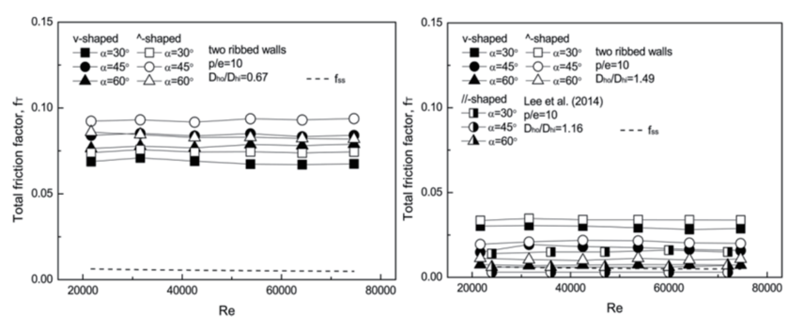

Fig. 4. Total friction factors

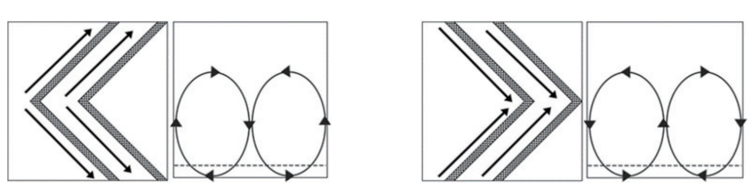

a) V-shaped b) Λ-shaped

Fig. 5. Schematic views of secondary flows

Our previous work [7] with in-line parallel angled ribs (//; 30°, 45°, and 60°) on the two opposite walls of D_{ho}/D_{hi} =1.16 provides much lower total friction factors than in the present Λ/V-shaped ribbed wall channels with flow attack angles of 30°, 45°, and 60°. It is reasoned that the more serious main stream flow blocking may be experienced in the present Λ/V-shaped ribs rather than the parallel angled ribs (//-shaped) because of the divided turbulent swirls as shown in Fig. 5.

Figure 6 represents the local streamwise heat transfer coefficients for the V-shaped ribs with three different flow attack angles of 30°, 45°, and 60° in the two opposite in-line ribbed convergent /divergent channel. In the ribs of flow attack angle of 30° and 45° at D_{ho}/D_{hi} =1.49, the local heat transfer coefficient h decreases from the highest value at the entrance with increasing streamwise distance; however, for the other ribs the local heat transfer coefficient shows somewhat constant values along the streamwise distance except around the outlet of test section.

This suggests that the V-shaped ribs may produce the secondary flow, and therefore promote more strongly the local convective heat transfer coefficient in the divergent channel with the flow attack angles of 30° and 45°.

For the divergent channel (D_{ho}/D_{hi} =1.49), the heat transfer coefficient diminishes after around x/D_h = 6. It is reasoned that the secondary flow from the V-shaped ribs on the opposite side wall shown in Fig. 5 may promote the turbulent flow in the channel.

The local heat transfer coefficients for the Λ-shaped ribs with three different flow attack angles of 30°, 45°, and 60° in the two opposite in-line ribbed convergent /divergent channel are shown in Fig.7.

The different streamwise variation patterns of the local convective heat transfer coefficients between the ribbed convergent channel shown in Fig. 6 and the ribbed divergent channel shown in Fig.7 are evidently caused by the fact that 1) the streamwise flow is accelerated/decelerated in the convergent/divergent channel, 2) the ribs are oriented to create a secondary flow that moves along the rib axes from the edge to center side in the Λ-shaped ribs; whereas, from the center to edge side in the V-shaped ribs.

For the Λ-shaped ribs with flow attack angle (α) of 30°, the peak of local heat transfer coefficient in the ribbed divergent channel locates much earlier than in the ribbed convergent one. This advance of peak in the ribbed divergent channel is

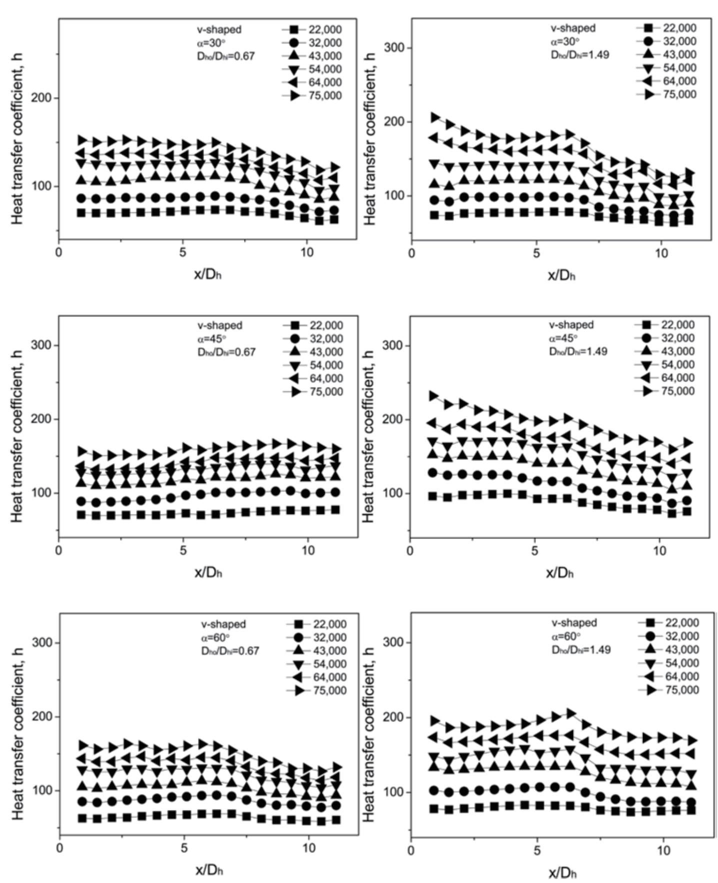

Fig. 6. Local streamwise heat transfer coefficients for V-shaped ribs

due to the stronger flow recirculation.

The Reynolds number dependencies of the dimensionless channel average Nusselt number (Nu/Nu_{ss}) for three different angled V / Λ-shaped ribs are presented in Fig. 8, along with results by Ref. [4]. The Nusselt numbers are normalized by the Dittus-Boelter's correlations Nu_{ss} for the fully developed smooth tubes as a reference.

In the V-shaped ribs (solid symbols), the higher dimensionless Nusselt numbers are exhibited in the divergent channel (D_{ho}/D_{hi} = 1.49) rather than in the convergent channel (D_{ho}/D_{hi} = 0.67); whereas, in the Λ-shaped ribs (open symbols), somewhat higher dimensionless Nusselt numbers are produced in the convergent channel (D_{ho}/D_{hi} = 0.67).

This is the contrary to the public opinion in the divergent channel that the heat transfer coefficient is usually proportional to the flow velocity.

This is resulted from the flow deceleration in the V-shaped ribs of D_{ho}/D_{hi} = 1.49, which produces the air bulk temperature increase and leads to an increase in the Nusselt number to some extent.

The present dimensionless Nusselt numbers in the ribbed convergent/divergent channel are somewhat greater than

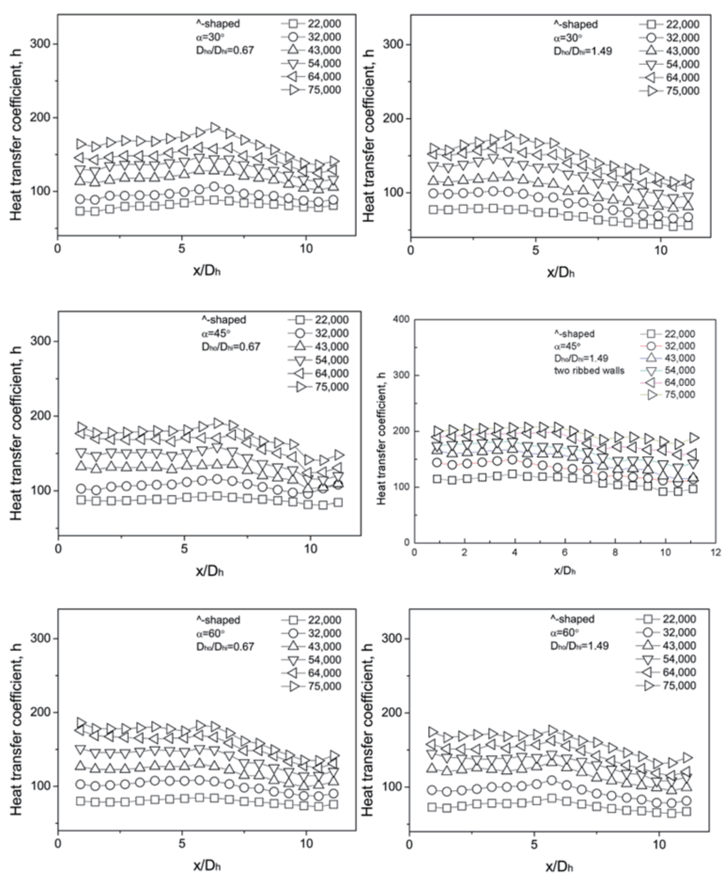

Fig. 7. Local streamwise heat transfer coefficients for Λ-shaped ribs

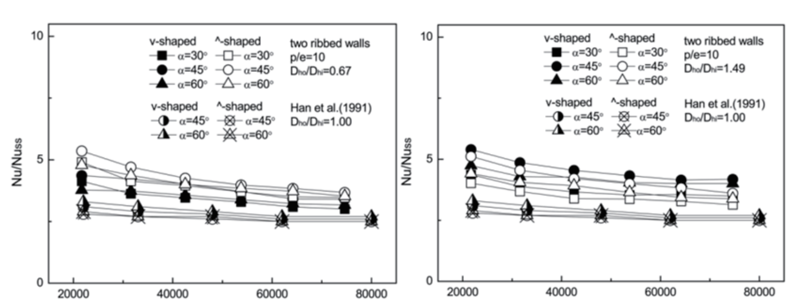

Fig. 8. Dimensionless Nusselt numbers

those for Han et al. [4], in which two opposite ribbed straight square channel of D_{ho}/D_{hi}=1.0 along the streamwise distance is placed and all four walls are heated in the test section.

This occurs because 1) the cold fluids from the two unheated walls move toward the two heated walls in the present work, 2) the dynamic pressure drops are produced in the convergent/divergent channel.

The 45° and Λ-shaped rib (solid circle) in the convergent channel and 45° and V-shaped rib (open circle) in the divergent channel produce the greatest dimensionless Nusselt numbers, respectively.

Attention is now turned to the relative thermal performance of the different ribbed convergent/divergent channels under the constraint of identical pumping power condition.

Identical pumping power is given by,

$$(\frac{\dot{m}}{\rho}\Delta P)^{*} = (\frac{\dot{m}}{\rho}\Delta P), \tag{5}$$

where the superscript * indicates the compared channel and the quantity without * is the reference channel (straight smooth circular tube). From Eq. (6), the following formula is obtained by,

$$(ARe^3 f/D_h^3\ )^{*} = \ (ARe^3 f/D_h^3)\ . \tag{6}$$

And Eq. (6) can be also presented in terms of the following Reynolds number,

$$Re = \sqrt[3]{(\frac{Re^3\ f\ A}{D_h^3})/(^{fA}/_{D_h^3})^{*}}\ . \tag{7}$$

Under the condition of the equivalent temperature

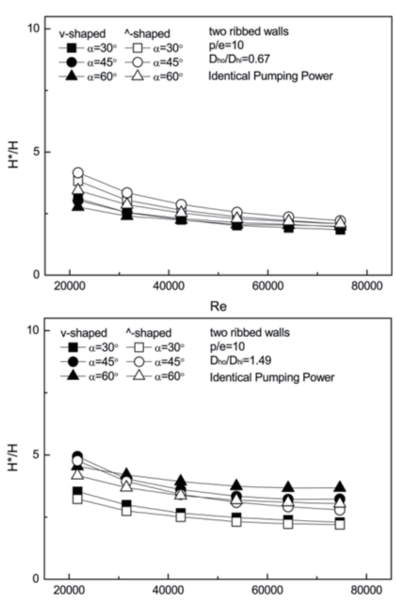

Fig. 9. Thermal Performance

different between the fluid and the wall, the ratio of the heat transfer between the compared channel and reference may be formulated as follows,

$$\frac{H^*}{H} = \frac{[Nu(Re)]^*}{Nu(Re)}, \tag{8}$$

where $Nu(Re)$ shows the experimental correlation between the Nusselt number and the Reynolds number for the straight circular smooth tube.

The comparisons of the channel average heat transfer performance for the convergent/divergent channel are indicated in Fig. 9. It can be observed in Fig. 9 that the ribbed divergent channels have greater thermal performance that those of the ribbed convergent channels. And the Λ-shaped ribs exhibit higher thermal performance than the V-shaped ribs in the convergent channel; whereas, the V-shaped ribs produce the higher thermal performance in the divergent channel.

In the convergent channel, the 45° with Λ-shaped rib is the best at all the Reynolds numbers studied, while in the divergent channel, the 60° with V-shaped rib is the best over the Reynold number of 30,000.

5. Conclusions

The work reported here is a systematic experimental study of the convergent/divergent channels with ribs of Λ/V-shape and three different flow attack angles (30°, 45°, and 60°). The major findings are as follows:

1) The negative (-) total pressure drops (ΔP_T) are produced in all cases in the convergent channel; whereas, the positive (+) total pressure drops in the divergent channel are attributed to due to the increased magnitude of dynamic pressure drop.

2) In the V-shaped ribs (solid symbols), the higher dimensionless Nusselt numbers are exhibited in the divergent channel (D_{ho}/D_{hi} =1.49) rather than D_{ho}/D_{hi} =0.67; whereas, in the Λ-shaped ribs (open symbols), somewhat higher dimensionless Nusselt numbers are produced in the convergent channel (D_{ho}/D_{hi} =0.67).

3) Under the constraints of at the identical pumping power, the 45° with Λ-shaped rib is the best thermal performance in the convergent channel at all the Reynolds numbers studied; whereas, the 60° with V-shaped rib is the best over the Reynold number of 30,000 in the divergent channel.

References

[1] Ahn, S. W., Kang, H. K., Bae, S. T. and Lee, D. H., "Heat Transfer and Friction Factor in a Square Channel

with One, Two, or Four Inclined Ribbed Walls", *ASME J. Turbomachinery*, Vol. 130, 2008, pp. 034501-5.

[2] Han, J. C., "Heat Transfer and Friction in Channels with Two Opposite Rib-Roughened Walls", *ASME J. Heat Transfer*, Vol. 106, 1984, pp. 774-781.

[3] Han, J. C., Glickman, L. R. and Rohsenow, W. M., "An Investigation of Heat Transfer and Friction for Rib-Roughened Surface", *International Journal of Heat and Mass Transfer*, Vol. 21, 1978, pp. 1143-1156.

[4] Han, J. C., Zhang, Y. M. and Lee, C. L., "Augmented Heat Transfer in Square Channels with Parallel, Crossed, and V-shaped Angled Ribs", *ASME J. Heat Transfer*, Vol. 113, 1991, pp. 590-596.

[5] Lee, M. S., Jeong, S. S., Ahn, S. W. and Han, J. C., "Heat Transfer and Friction in the Rectangular Convergent and Divergent Channels with Ribs", *AIAA Journal of Thermophysics and Heat Transfer*, Vol. 27, 2013, pp. 660-667.

[6] Lee, M. S. and Ahn, S. W., "Heat Transfer and Frictions in the Rectangular Channel with Ribs on One Wall", *International Journal of Aeronautical and Space Science*, Vol. 17, 2016, pp. 351-356.

[7] Lee, M. S., Jeong, S. S., Ahn, S. W. and Han, J. C., "Effects of Angled Ribs on Turbulent Heat Transfer and Friction Factors in a Rectangular Divergent Channel", *International Journal of Thermal Science*, Vol. 84, 2014, pp. 1-8.

[8] Kline, S. J. and McClintock, F. A., "Describing Uncertainties in Single Sample Experiments", *Mechanical Engineering*, Vol. 75, 1953, pp. 3-8.

[9] White, F. M., *Viscous Fluid Flow*, McGraw-Hill Inc., New York, 1991, pp. 394-499.

DOI: http://dx.doi.org/10.5139/IJASS.2017.18.3.395